Planetary Gear Modeling Using the Power-Oriented Graphs Technique.

Roberto Zanasi, Davide Tebaldi

***Abstract*— In this paper, the Power-Oriented Graphs (POG) technique is used to model Planetary Gear transmission systems. The full elastic dynamic model of the system is obtained using a fast and direct method which can be easily applied to any type of planetary gear. The rigid and reduced dynamic model of the system when the stiffness coefficients go to infinity is then obtained using a POG congruent state space transformation allowing the user to select which angular speeds are to be maintained in the reduced model. Another interesting aspect of the presented method is that the obtained reduced model is still able to provide the time behaviors of the tangential forces present between each couple of gears of the considered planetary gear system. The presented fast and direct method is then applied to two practical case studies, and simulative results in Matlab/Simulink showing the effectiveness of the method are finally reported and commented.**

I. Introduction

Planetary gear transmission systems are amply used in several applications, including the design of new hybrid architectures in the automotive and agricultural fields, where such elements play a fundamental role as power-split devices. The need of providing direct and accurate dynamic planetary gear models is therefore becoming more and more important, in order to investigate the system behavior in all its aspects. In [1], the authors mainly focus on the design part of planetary gear systems. In [2], the authors propose the usage of the lumped parameter dynamic model for modeling planetary gears; whereas in [3], the authors model the rigid gear subsystem, composed of a sun gear, the planet gears and a planet carrier, by using a lumped parameter model, and the elastic ring gear subsystem by using a finite element model. The problem of the dynamic modeling of a planetary gear system is also addressed by the authors in [4]. In this latter paper, the authors focus on the modeling of a specific type of planetary gear by using the classical state-space approach. An automated approach for modeling planetary gears is proposed by the authors in [5]. In this study, the classical state-space approach is once again adopted.

In this paper, we propose a direct and systematic method to model planetary gear systems using the Power-Oriented Graphs technique, see [6]. The proposed method makes it possible to model any type of planetary gear system by also considering the translational springs being present among the gears. In addition, the user-friendly graphical representation of the POG modeling technique provides the user with a quick understanding of the system dynamic equations. The use of the POG state-space model rather than the classical state-space approach brings several advantages, among which we can mention the potentiality of applying a congruent state-space transformation allowing to reduce the order of the system. Indeed, the study presented in this paper shows that, when the stiffness coefficients go to infinity, the reduced rigid model can be obtained by using a POG congruent state space transformation. From the reduced rigid model, it is also possible to obtain the tangential forces associated with the elastic elements of the full elastic model.

Roberto Zanasi and Davide Tebaldi are with the Department of Engineering "Enzo Ferrari", University of Modena and Reggio Emilia, Modena, Italy, e-mail: roberto.zanasi@unimore.it, davide.tebaldi@unimore.it

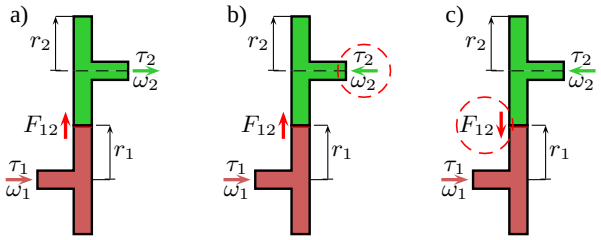

Fig. 1. Gear transmission: positive directions of the system variables.

The paper is organized as follows: In Sec. II, we focus on the modeling of a gear transmission. In Sec. III, we generalize the rules presented in Sec. II in order to describe the systematic approach for modeling planetary gears allowing to compute the radius matrix, which fully defines the planetary gear under consideration. Additionally, we apply the presented systematic modeling approach to a one-stage planetary gear. In Sec. IV, we focus on a more complex case study: the modeling of a two-stages planetary gear. Finally, Sec. V illustrates the conclusions of the work presented in this paper.

II. Modeling a gear transmission

Let us consider the gear transmission shown in Fig. 1 case a). The figure highlights the positive directions of the system variables: the angular velocities of the two gears, ω_1 and ω_2, together with the tangential force F_{12} that gear 1 transmits to gear 2. The POG block scheme of the gear transmission in Fig. 1 case a) is shown in Fig. 2 and the corresponding POG state space equations are reported in (1).

$$\begin{cases} \underbrace{\left[\begin{array}{cc|c} J_1 & 0 & 0 \\ 0 & J_2 & 0 \\ \hline 0 & 0 & K^{-1} \end{array}\right]}_{\mathbf{L}} \dot{\mathbf{x}} = \underbrace{\left[\begin{array}{cc|c} -b_1 & 0 & -r_1 \\ 0 & -b_2 & -r_2 \\ \hline r_1 & r_2 & 0 \end{array}\right]}_{\mathbf{A}} \underbrace{\left[\begin{array}{c} \omega_1 \\ \omega_2 \\ \hline F_{12} \end{array}\right]}_{\mathbf{x}} + \underbrace{\left[\begin{array}{cc} 1 & 0 \\ 0 & 1 \\ \hline 0 & 0 \end{array}\right]}_{\mathbf{B}} \underbrace{\left[\begin{array}{c} \tau_1 \\ \tau_2 \end{array}\right]}_{\mathbf{u}} \\ \underbrace{\left[\begin{array}{c} \omega_1 \\ \omega_2 \end{array}\right]}_{\mathbf{y}} = \underbrace{\left[\begin{array}{cc|c} 1 & 0 & 0 \\ 0 & 1 & 0 \end{array}\right]}_{\mathbf{C}} \mathbf{x} + \underbrace{\left[\begin{array}{cc} 0 & 0 \\ 0 & 0 \end{array}\right]}_{\mathbf{D}} \mathbf{u} \end{cases} \quad (1)$$

The meaning of the parameters within system (1) is the

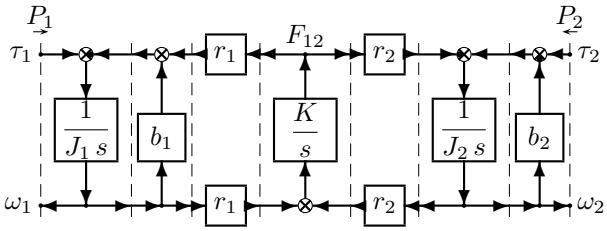

Fig. 2. POG block scheme of a considered gear transmission.

following: J_1, b_1 and r_1 are the moment of inertia, the linear friction coefficient and the radius of the first gear. Equivalently, parameters J_2, b_2 and r_2 are the moment of inertia, the linear friction coefficient and the radius of the second gear, whereas parameter K is the stiffness of the contact spring between the first and the second gear. The signs of the parameters within system (1) and Fig. 2 are a direct consequence of the choices about the positive direction of the system state variables ω_1, ω_2 and F_{12}. Powers $P_1 = \omega_1\, \tau_1$ and $P_2 = \omega_2\, \tau_2$ flowing through the input and output power sections are positive, see Fig. 2, if they are entering the system, meaning that the positive directions of the input torques τ_1 and τ_2 have been chosen to be equal to the positive directions of the angular velocities ω_1 and ω_2. One can easily prove that, if the positive direction of variables ω_2 and τ_2 is reversed, see Fig. 1 case b), the state space equations remain the same except for matrix $\mathbf{A}$, which turns into:

$$\mathbf{A}_1 = \left[\begin{array}{cc|c} -b_1 & 0 & -r_1 \\ 0 & -b_2 & r_2 \\ \hline r_1 & -r_2 & 0 \end{array}\right].$$

In this case, only the sign of parameter r_2 is changed. Moreover, by starting from case b) and reversing the positive direction of variable F_{12}, see Fig. 1 case c), the state space equations (1) remain unchanged once again except for matrix $\mathbf{A}$, which now turns into:

$$\mathbf{A}_2 = \left[\begin{array}{cc|c} -b_1 & 0 & r_1 \\ 0 & -b_2 & -r_2 \\ \hline -r_1 & r_2 & 0 \end{array}\right]$$

In this case, the signs of both parameters r_1 and r_2 within matrix $\mathbf{A}_2$ are changed with respect to matrix $\mathbf{A}_1$. By rewriting matrix $\mathbf{A}$ in the following form:

$$\mathbf{A} = \begin{bmatrix} -\mathbf{B}_J & \mathbf{R}^{\mathrm{T}} \\ \mathbf{R} & 0 \end{bmatrix}, \qquad \mathbf{B}_J = \begin{bmatrix} b_1 & 0 \\ 0 & b_2 \end{bmatrix}, \qquad \mathbf{R} = \begin{bmatrix} r_1 & r_2 \end{bmatrix}$$

and focusing on the previous two cases, one can state that: 1) matrix $\mathbf{B}_J$ does not change even if the system variables ω_1, ω_2 and F_{12} change the signs of their positive directions; 2) if the angular velocity ω_i changes the sign of its positive direction, then all the coefficients of the i-th column of matrix $\mathbf{R}$ change their signs; 3) if the tangential force F_{12} changes the sign of its positive direction, then all the coefficients of matrix $\mathbf{R}$ change their signs.

III. Modeling a one-stage planetary gear

Reference is made to the planetary gear shown in Fig. 3. Within the figure, each gear is characterized by a one-digit

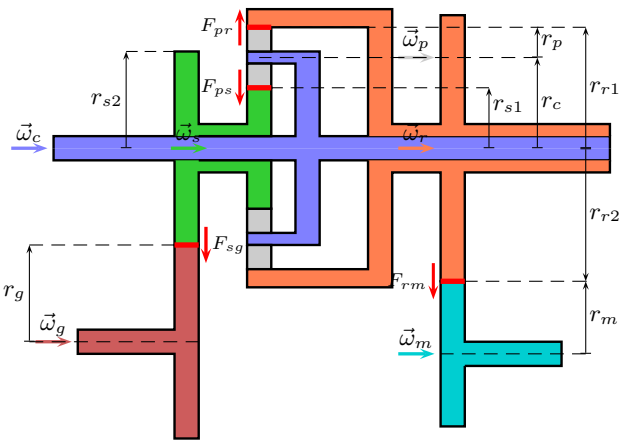

Fig. 3. Basic structure of the considered one-stage planetary gear.

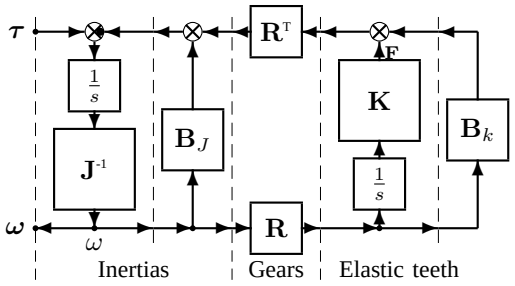

Fig. 4. POG scheme of the considered planetary gear system.

subscript "i", where $i \in \{c, p, s, r, g, m\}$, and a specific color. Each gear rotates around a horizontal axis, denoted in the figure by a short arrow (i.e. "→"), having the same color of the considered gear. The direction of the short arrow indicates the positive direction of the associated angular velocity $\vec{\omega}_i$ of gear "i". The one-digit string "i" also denotes all the parameters and variables associated with gear "i": J_i is the moment of inertia, b_i is the linear friction coefficient and τ_i is the input torque applied to the gear.

The gears interact each other by means of their teeth. The contact points of the gears are denoted in Fig. 3 by short red lines (i.e. "▬") representing the stiffness of the teeth where the gears interact each other. The tangential forces F_{ij} transmitted by the contact points are denoted in Fig. 3 by short red vertical arrows (i.e. " ↓ ") representing the positive directions of the contact forces themselves. The two-digits subscript "ij" of the tangential force F_{ij} indicates that such force is positive if oriented from gear "i" to gear "j" and that the spring connecting the two gears has its first terminal connected to gear "i" and its second terminal connected to gear "j". Such two-digits string also denotes all the parameters and variables associated with the spring "ij": K_{ij} is the spring stiffness and b_{ij} is the spring linear friction coefficient.

The dynamic equations of the considered system are graphically represented by the POG scheme shown in Fig. 4. The corresponding state space equations are:

$$\begin{cases} \mathbf{L}\,\dot{\mathbf{x}} = \mathbf{A}\,\mathbf{x} + \mathbf{B}\,\mathbf{u} \\ \mathbf{y} = \mathbf{B}^{\mathrm{T}}\,\mathbf{x} \end{cases}, \qquad \mathbf{x} = \begin{bmatrix} \boldsymbol{\omega} \\ \mathbf{F} \end{bmatrix}, \qquad \mathbf{B} = \begin{bmatrix} \mathbf{I} \\ \mathbf{0} \end{bmatrix} \qquad (2)$$

where $\mathbf{x}$, $\mathbf{u} = \boldsymbol{\tau}$, $\mathbf{y} = \boldsymbol{\omega}$ are the state, input and output vectors of the system, respectively, $\mathbf{B}$ is the input matrix and $\mathbf{I}$ is an identity matrix of proper dimension. The energy and power matrices $\mathbf{L}$ and $\mathbf{A}$ have the following structure:

$$\mathbf{L} = \begin{bmatrix} \mathbf{J} & \mathbf{0} \\ \mathbf{0} & \mathbf{K}^{-1} \end{bmatrix}, \quad \mathbf{A} = \begin{bmatrix} -\mathbf{B}_J - \mathbf{R}^{\mathrm{T}}\mathbf{B}_k\mathbf{R} & -\mathbf{R}^{\mathrm{T}} \\ \mathbf{R} & \mathbf{0} \end{bmatrix} \quad (3)$$

The velocity vector $\boldsymbol{\omega}$, the input torque vector $\boldsymbol{\tau}$ and the force vector $\mathbf{F}$ are defined as follows:

$$\boldsymbol{\omega} = \begin{bmatrix} \omega_c \\ \omega_p \\ \omega_s \\ \omega_r \\ \omega_g \\ \omega_m \end{bmatrix}, \quad \boldsymbol{\tau} = \begin{bmatrix} \tau_c \\ \tau_p \\ \tau_s \\ \tau_r \\ \tau_g \\ \tau_m \end{bmatrix}, \quad \mathbf{F} = \begin{bmatrix} F_{ps} \\ F_{pr} \\ F_{sg} \\ F_{rm} \end{bmatrix}. \quad (4)$$

The inertia matrix $\mathbf{J}$ and the inertia friction matrix $\mathbf{B}_J$ are:

$$\mathbf{J} = \begin{bmatrix} J_c & 0 & 0 & 0 & 0 & 0 \\ 0 & J_p & 0 & 0 & 0 & 0 \\ 0 & 0 & J_s & 0 & 0 & 0 \\ 0 & 0 & 0 & J_r & 0 & 0 \\ 0 & 0 & 0 & 0 & J_g & 0 \\ 0 & 0 & 0 & 0 & 0 & J_m \end{bmatrix}, \quad \mathbf{B}_J = \begin{bmatrix} b_c & 0 & 0 & 0 & 0 & 0 \\ 0 & b_p & 0 & 0 & 0 & 0 \\ 0 & 0 & b_s & 0 & 0 & 0 \\ 0 & 0 & 0 & b_r & 0 & 0 \\ 0 & 0 & 0 & 0 & b_g & 0 \\ 0 & 0 & 0 & 0 & 0 & b_m \end{bmatrix}.$$

The stiffness matrices $\mathbf{K}$ and $\mathbf{B}_K$ are defined as follows:

$$\mathbf{K} = \begin{bmatrix} K_{ps} & 0 & 0 & 0 \\ 0 & K_{pr} & 0 & 0 \\ 0 & 0 & K_{sg} & 0 \\ 0 & 0 & 0 & K_{rm} \end{bmatrix}, \quad \mathbf{B}_K = \begin{bmatrix} b_{ps} & 0 & 0 & 0 \\ 0 & b_{pr} & 0 & 0 \\ 0 & 0 & b_{sg} & 0 \\ 0 & 0 & 0 & b_{rm} \end{bmatrix}.$$

The position of the angular velocities ω_i within vector $\boldsymbol{\omega}$ and of the tangential forces F_{ij} within vector $\mathbf{F}$, see (4), completely and uniquely defines the position of parameters J_i, b_i, K_{ij} and b_{ij} within diagonal matrices $\mathbf{J}$, $\mathbf{B}_J$, $\mathbf{K}$ and $\mathbf{B}_K$ respectively. The only matrix in Fig. 3 and in the state space equations (2) that fully defines the internal structure of the given planetary gear is the radius matrix $\mathbf{R}$. As far as the considered system is concerned, matrix $\mathbf{R}$ is defined as:

$$\mathbf{R} = \begin{bmatrix} r_c & -r_p & -r_{s1} & 0 & 0 & 0 \\ r_c & r_p & 0 & -r_{r1} & 0 & 0 \\ 0 & 0 & -r_{s2} & 0 & -r_g & 0 \\ 0 & 0 & 0 & -r_{r2} & 0 & -r_m \end{bmatrix}. \quad (5)$$

The radii present in matrix $\mathbf{R}$ are defined in Fig. 3 and are constrained as follows: $r_c = r_p + r_{s1}$ and $r_{r1} = 2r_p + r_{s1}$.

A. Direct derivation of the radius matrix R.

Let $r_{ij,i}$ denote the generic coefficient of matrix $\mathbf{R} = [r_{ij,i}]$ in (5). Subscripts $ij \in \{ps, pr, sg, rm\}$ and $i \in \{c, p, s, r, g, m\}$ indicate that $r_{ij,i}$ is the coefficient that links the tangential force $\vec{F}_{ij}$ to the angular velocity $\vec{\omega}_i$. Generalizing the rules provided at the end of Sec. II, one can easily prove that coefficient $r_{ij,i}$ can be expressed as:

$$r_{ij,i} = S_{F_{ij}}\, S_{\omega_i}\, r_i$$

where r_i, $S_{F_{ij}}$ and S_{ω_i} have the following meaning:

1) r_i is the *effective radius* of angular velocity $\vec{\omega}_i$. Two different cases must be considered: a) if velocity $\vec{\omega}_i$ directly affects the force vector $\vec{F}_{ij}$, see Fig. 5.a, then the *effective radius* r_i coincides with the radius of the gear associated with velocity $\vec{\omega}_i$; b) if angular velocity $\vec{\omega}_i$ affects the force vector $\vec{F}_{ij}$ through an intermediate gear "j", see Fig. 5.b, then the *effective radius* r_i coincides with the distance between the rotation axes of the two angular velocities $\vec{\omega}_i$ and $\vec{\omega}_j$.

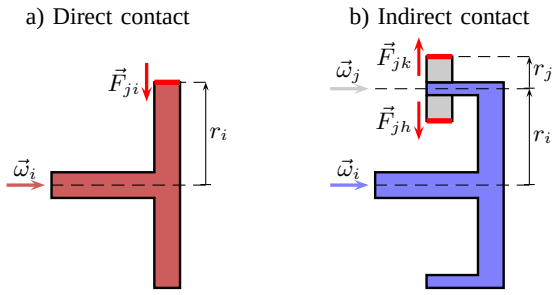

Fig. 5. *Effective radius* r_i: a) Direct contact; b) Indirect contact.

2) $S_{F_{ij}}$ is the sign of the positive direction of vector $\vec{F}_{ij}$:

$$S_{F_{ij}} = \begin{cases} 1 & \text{if } \vec{F}_{ij} \text{ is oriented from gear } i \text{ to gear } j \\ -1 & \text{if } \vec{F}_{ji} \text{ is oriented from gear } j \text{ to gear } i \end{cases}$$

3) S_{ω_i} is related to the sign of the velocity vector $\vec{\omega}_i$:

$$S_{\omega_i} = \begin{cases} 1 & \text{if } \vec{F}_{ij} \text{ is on the left of vector } \vec{\omega}_i \\ -1 & \text{if } \vec{F}_{ij} \text{ is on the right of vector } \vec{\omega}_i \end{cases}$$

The left and right sides of vector $\vec{\omega}_i$ are determined by moving in the positive direction along vector $\vec{\omega}_i$.

Applying the previous rules to the gears shown in Fig. 5, it results: a) coefficient $r_{ij,i}$ associated with the direct contact of case a) is $r_{ij,i} = -r_i$ because $S_{F_{ji}} = -1$ and $S_{\omega_i} = 1$; b) coefficients $r_{jk,i}$ and $r_{jh,i}$ associated with the indirect contacts of case b) are $r_{jk,i} = r_{jh,i} = r_i$ because $S_{F_{jh}} = S_{F_{jk}} = 1$ and $S_{\omega_i} = 1$.

From (2), it follows that $\dot{x}_{ij} = r_{ij,i}\,\omega_i$ is the tangential velocity of one of the two terminals of spring K_{ij} when the angular velocity $\vec{\omega}_i$ moves along its positive direction. Since the sign of velocity $\dot{x}_{ij}$ directly affects the sign of the force vector $\vec{F}_{ij}$, it is evident that $\dot{x}_{ij}$ must change sign both when the velocity vector $\vec{\omega}_i$ and when the force vector $\vec{F}_{ij}$ change their positive directions. Finally, Fig. 6 graphically shows why the *effective radius* of an angular velocity $\vec{\omega}_i$ is equal to r_i for both case a) and b) of direct and indirect contact. In particular, in the indirect contact case b) the tangential velocity $\dot{x}_{ij} = r_i\,\omega_i$ is the same for the two elastic elements K_{jh} and K_{jk} because, when $\vec{\omega}_i$ moves along its positive direction, the angular velocity $\vec{\omega}_j$ is kept equal to zero.

B. Rigid and reduced model when $\mathbf{K} \to \infty$.

When $\mathbf{K} \to \infty$, from state space model (2) one obtains:

$$\mathbf{R}\,\boldsymbol{\omega} = \mathbf{0} \quad \Leftrightarrow \quad \begin{cases} r_c\,\omega_c - r_p\,\omega_p - r_{s1}\,\omega_s = 0 \\ r_c\,\omega_c + r_p\,\omega_p - r_{r1}\,\omega_r = 0 \\ -r_g\,\omega_g - r_{s2}\,\omega_s = 0 \\ -r_m\,\omega_m - r_{r2}\,\omega_r = 0 \end{cases} \quad (6)$$

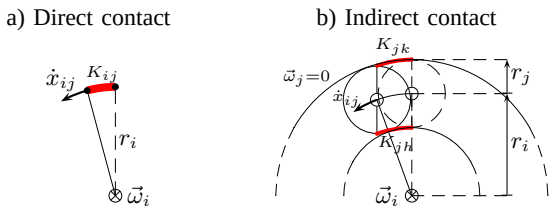

Fig. 6. Angular velocities $\vec{\omega}_i$ and tangential velocities $\dot{x}_{ij}$.

System (6) provides four static constraints between the six components ω_i of the angular velocity vector $\boldsymbol{\omega}$, meaning that vector $\boldsymbol{\omega}$ can be expressed as a function of "two" of the six composing angular velocities: $\boldsymbol{\omega} = \mathbf{Q}_1\mathbf{x}_1$, where $\mathbf{x}_1 = \begin{bmatrix}\omega_i & \omega_j\end{bmatrix}^{\mathrm{T}}$. By choosing $\mathbf{x}_1 = \begin{bmatrix}\omega_c & \omega_r\end{bmatrix}^{\mathrm{T}}$, one obtains the following congruent state space transformation:

$$\underbrace{\begin{bmatrix}\boldsymbol{\omega}\\ \mathbf{F}\end{bmatrix}}_{\mathbf{x}} = \begin{bmatrix}\omega_c\\ \omega_p\\ \omega_s\\ \omega_r\\ \omega_g\\ \omega_m\\ \hline F_{ps}\\ F_{pr}\\ F_{sg}\\ F_{rm}\end{bmatrix} = \underbrace{\left[\begin{array}{cc} 1 & 0\\ -\frac{r_c}{r_p} & \frac{r_{r1}}{r_p}\\ \frac{2r_c}{r_{s1}} & -\frac{r_{r1}}{r_{s1}}\\ 0 & 1\\ -\frac{2r_c r_{s2}}{r_g r_{s1}} & \frac{r_{r1} r_{s2}}{r_g r_{s1}}\\ 0 & -\frac{r_{r2}}{r_m}\\ \hline 0 & 0\\ 0 & 0\\ 0 & 0\\ 0 & 0 \end{array}\right]}_{\mathbf{T}_1} \underbrace{\begin{bmatrix}\omega_c\\ \omega_r\end{bmatrix}}_{\mathbf{x}_1} = \underbrace{\begin{bmatrix}\mathbf{Q}_1\\ \mathbf{0}\end{bmatrix}}_{\mathbf{T}_1}\mathbf{x}_1.$$

By applying transformation $\mathbf{x} = \mathbf{T}_1\mathbf{x}_1$ to system (2), one obtains the following reduced system $\mathbf{L}_1\dot{\mathbf{x}}_1 = \mathbf{A}_1\mathbf{x}_1 + \mathbf{B}_1\mathbf{u}$:

$$\underbrace{\begin{bmatrix} J_1 & J_3\\ J_3 & J_2\end{bmatrix}}_{\mathbf{L}_1}\underbrace{\begin{bmatrix}\dot{\omega}_c\\ \dot{\omega}_r\end{bmatrix}}_{\dot{\mathbf{x}}_1} = \underbrace{\begin{bmatrix} b_1 & b_3\\ b_3 & b_2\end{bmatrix}}_{\mathbf{A}_1}\underbrace{\begin{bmatrix}\omega_c\\ \omega_r\end{bmatrix}}_{\mathbf{x}_1} + \underbrace{\mathbf{Q}_1^{\mathrm{T}}}_{\mathbf{B}_1}\underbrace{\boldsymbol{\tau}}_{\mathbf{u}} \qquad (7)$$

where martices $\mathbf{L}_1$, $\mathbf{A}_1$ and $\mathbf{B}_1$ have the following structure:

$$\begin{cases} \mathbf{L}_1 = \mathbf{T}_1^{\mathrm{T}}\mathbf{L}\,\mathbf{T}_1 = \mathbf{Q}_1^{\mathrm{T}}\mathbf{J}\,\mathbf{Q}_1\\ \mathbf{A}_1 = \mathbf{T}_1^{\mathrm{T}}\mathbf{A}\,\mathbf{T}_1 = -\underbrace{\mathbf{Q}_1^{\mathrm{T}}\mathbf{R}^{\mathrm{T}}\mathbf{B}_K\mathbf{R}\,\mathbf{Q}_1}_{\mathbf{0}} - \mathbf{Q}_1^{\mathrm{T}}\mathbf{B}_J\mathbf{Q}_1\\ \mathbf{B}_1 = \mathbf{T}_1^{\mathrm{T}}\mathbf{B} = \mathbf{Q}_1^{\mathrm{T}}\end{cases}$$

Term $\mathbf{Q}_1^{\mathrm{T}}\mathbf{R}^{\mathrm{T}}\mathbf{B}_K\mathbf{R}\mathbf{Q}_1$ is equal to zero because $\mathbf{Q}_1 \in \mathrm{Ker}(\mathbf{R})$:

$$\mathbf{R}\,\boldsymbol{\omega} = \mathbf{0} \quad \Leftrightarrow \quad \mathbf{R}\,\mathbf{Q}_1\,\mathbf{x}_1 = \mathbf{0} \quad \Leftrightarrow \quad \mathbf{R}\,\mathbf{Q}_1 = \mathbf{0}.$$

The structure of elements J_1, J_3 and J_2 in matrix $\mathbf{L}_1$ is:

$$\begin{aligned} J_1 &= J_c + \frac{J_p {r_c}^2}{{r_p}^2} + \frac{4J_s {r_c}^2}{{r_{s1}}^2} + \frac{4J_g {r_c}^2 {r_{s2}}^2}{{r_g}^2 {r_{s1}}^2}\\ J_3 &= -\frac{J_p r_c r_{r1}}{{r_p}^2} - \frac{2J_s r_c r_{r1}}{{r_{s1}}^2} - \frac{2J_g r_c r_{r1} r_{s2}}{{r_g}^2 {r_{s1}}^2}\\ J_2 &= J_r + \frac{J_m {r_{r2}}^2}{{r_m}^2} + \frac{J_p {r_{r1}}^2}{{r_p}^2} + \frac{J_s {r_{r1}}^2}{{r_{s1}}^2} + \frac{J_g {r_{r1}}^2 {r_{s2}}^2}{{r_g}^2 {r_{s1}}^2}\end{aligned}$$

The structure of elements b_1, b_3 and b_2 in matrix $\mathbf{A}_1$ is:

$$\begin{aligned} b_1 &= -b_c - \frac{b_p {r_c}^2}{{r_p}^2} - \frac{4b_s {r_c}^2}{{r_{s1}}^2} - \frac{4b_g {r_c}^2 {r_{s2}}^2}{{r_g}^2 {r_{s1}}^2}\\ b_3 &= \frac{b_p r_c r_{r1}}{{r_p}^2} + \frac{2b_s r_c r_{r1}}{{r_{s1}}^2} + \frac{2b_g r_c r_{r1} r_{s2}}{{r_g}^2 {r_{s1}}^2}\\ b_2 &= -b_r - \frac{b_m {r_{r2}}^2}{{r_m}^2} - \frac{b_p {r_{r1}}^2}{{r_p}^2} - \frac{b_s {r_{r1}}^2}{{r_{s1}}^2} - \frac{b_g {r_{r1}}^2 {r_{s2}}^2}{{r_g}^2 {r_{s1}}^2}\end{aligned}$$

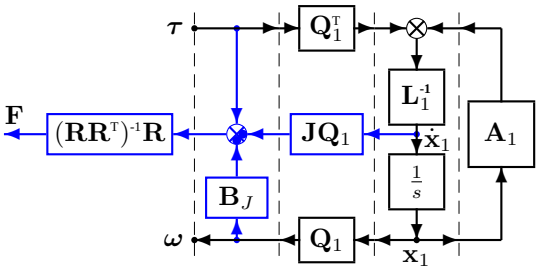

Fig. 7. Modified POG block scheme of the considered planetary gear.

Property 1. *The force vector* $\mathbf{F}$ *is not present in the reduced system (7), but its time behavior can still be obtained using the following relation:*

$$\mathbf{F} = (\mathbf{R}\mathbf{R}^{T})^{-1}\mathbf{R}(\boldsymbol{\tau} - \mathbf{J}\mathbf{Q}_1\dot{\mathbf{x}}_1 - \mathbf{B}_J\mathbf{Q}_1\mathbf{x}_1) \qquad (8)$$

Proof. From (2) and (7), one obtains:

$$\mathbf{R}^{\mathrm{T}}\mathbf{F} = \boldsymbol{\tau} - \mathbf{J}\,\dot{\boldsymbol{\omega}} - (\mathbf{B}_J + \mathbf{R}^{\mathrm{T}}\mathbf{B}_k\mathbf{R})\,\boldsymbol{\omega}$$

When $\mathbf{K} \to \infty$, it is $\boldsymbol{\omega} = \mathbf{Q}_1\mathbf{x}_1$. By substituting in the previous relation, it results:

$$\mathbf{R}^{\mathrm{T}}\mathbf{F} = \boldsymbol{\tau} - \mathbf{J}\,\mathbf{Q}_1\dot{\mathbf{x}}_1 - \mathbf{B}_J\mathbf{Q}_1\mathbf{x}_1 - \mathbf{R}^{\mathrm{T}}\mathbf{B}_k\underbrace{\mathbf{R}\mathbf{Q}_1}_{\mathbf{0}}\mathbf{x}_1. \qquad (9)$$

Relation (8) can be directly obtained from (9) by applying the pseudoinverse of matrix $\mathbf{R}$, that is $(\mathbf{R}\mathbf{R}^{\mathrm{T}})^{-1}\mathbf{R}$, on the left of relation (9) and recalling that $\mathbf{R}\mathbf{Q}_1 = \mathbf{0}$. □

The modified POG block scheme of Fig. 7 combines in the same figure the computation of the force vector $\mathbf{F}$ (blue blocks) with the POG reduced system (7) (black blocks).

C. Simulation results

Both the block scheme reported in Fig. 4, describing the full elastic model, and the one reported in Fig. 7, describing the reduced model, have been simulated in Matlab/Simulink using the following parameters and initial conditions:

```
r_s1 = 10*cm;              % Sun_1: radius
r_s2 = 16*cm;              % Sun_2: radius
r_p  = 4.8*cm;             % Planetary: radius
r_g  = 16*cm;              % Generator ring: radius
r_m  = 12*cm;              % Motor ring 1: radius
r_r2 = 22*cm;              % Motor ring 2: radius
r_c  = 14.8*cm;            % Carrier: radius
r_r1 = 19.6*cm;            % Ring: radius
J_c = 0.17648*kg*meters^2; % Carrier: inertia
J_p = 0.009756*kg*meters^2;% Planetary: inertia
J_r = 0.54251*kg*meters^2; % Ring: inertia
J_s = 0.038617*kg*meters^2;% Sun: inertia
J_g = 0.48197*kg*meters^2; % Generator: inertia
J_m = 0.15263*kg*meters^2; % Motor ring: inertia
b_c = 0.08*Nm/rpm;         % Carrier: friction coeff.
b_p = b_c; b_r = b_c; b_s = b_c; b_g = b_c; b_m = = b_c;
K_ps = 30*Newton/mm;       % Planetary-Sun: stiffness
K_pr = K_ps; K_sg = K_ps; K_rm = K_ps;
b_ps = 0.4*Newton*s/cm;    % Planetary-Sun: fric. coeff.
b_pr = b_ps; b_sg = b_ps; b_rm = b_ps;
Tau = [100 0 0 0 0 0]*Nm;  % Input Torques
W_0 = [0 0 0 0 0 0]*rpm;   % Angular velocities: In.Cond.
F_0 = [0 0 0 0]*Newton;    % Tangential forces: In.Cond.
```

The obtained simulation results are the following: the angular velocities ω_i, for $i \in \{c,\ p,\ s,\ r,\ g,\ m\}$, are shown in Fig. 8, and the tangential forces F_{ij}, for $ij \in \{ps,\ pr,\ sg,\ rm\}$, are shown in Fig. 9. The time behaviors plotted by using dashed

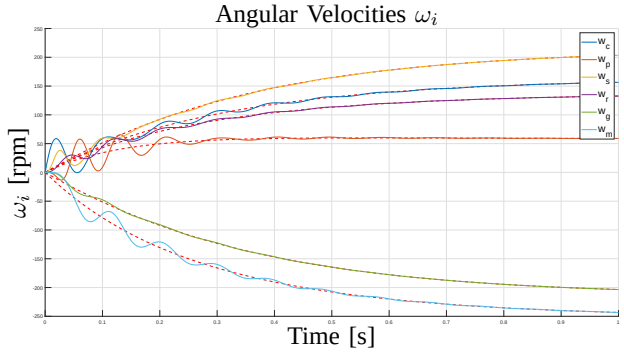

Fig. 8. Angular velocities ω_i, for $i \in \{c,\ p,\ s,\ r,\ g,\ m\}$.

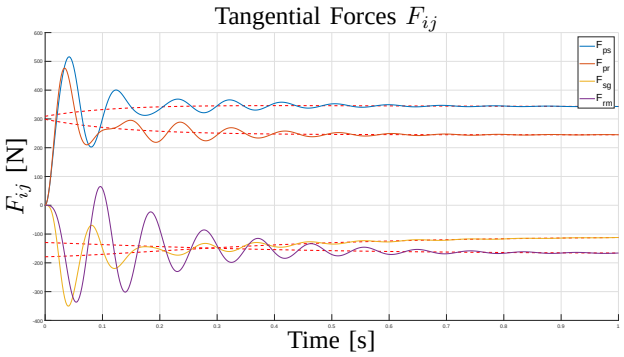

Fig. 9. Tangential forces F_{ij}, for $ij \in \{ps,\ pr,\ sg,\ rm\}$.

red lines refer to the simulation results obtained by using the rigid reduced system (7). The time behaviors plotted using colored lines refer to the simulation results obtained by using the extended POG system (2) taking the elasticities into account. From Fig. 8 and 9 it is evident that, after the transient, the time behaviors obtained by using the elastic model (2) asymptotically tend to those obtained by using the reduced model (7). Moreover, the time behaviors of the tangential forces F_{ij} corresponding to the reduced model (7) reported in Fig. 9 have been obtained by means of relation (8), giving a proof of the effectiveness of such relation.

IV. Modeling a Two-Stages Planetary Gear

Reference is made to the two-stages planetary gear shown in Fig. 10. The extended elastic model of the considered system can be graphically represented by using the POG scheme shown in Fig. 4 once again. The corresponding POG state space model can be obtained by means of the same equations and the same symbols used in (2) and in (3) for the previously considered one-stage planetary gear. As regards the two-stages planetary gear, the velocity vector $\boldsymbol{\omega}$, the input torque vector $\boldsymbol{\tau}$ the force vector $\mathbf{F}$ and the state vector $\mathbf{x}$ are defined as follows:

$$\boldsymbol{\omega} = \begin{bmatrix} \omega_s \\ \omega_c \\ \omega_p \\ \omega_a \\ \omega_r \\ \omega_b \\ \omega_q \end{bmatrix}, \quad \boldsymbol{\tau} = \begin{bmatrix} \tau_s \\ \tau_c \\ \tau_p \\ \tau_a \\ \tau_r \\ \tau_b \\ \tau_q \end{bmatrix}, \quad \mathbf{F} = \begin{bmatrix} F_{sp} \\ F_{sa} \\ F_{pr} \\ F_{ab} \\ F_{bq} \end{bmatrix}, \quad \mathbf{x} = \begin{bmatrix} \boldsymbol{\omega} \\ \mathbf{F} \end{bmatrix}.$$

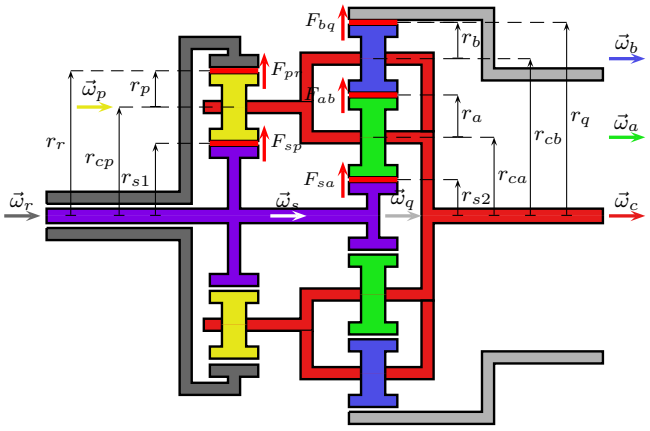

Fig. 10. Basic structure of the considered two-stages planetary gear.

In this case, the inertia and friction matrices $\mathbf{J}$ and $\mathbf{B}_J$ are:

$$\mathbf{J} = \begin{bmatrix} J_s & 0 & 0 & 0 & 0 & 0 & 0 \\ 0 & J_c & 0 & 0 & 0 & 0 & 0 \\ 0 & 0 & J_p & 0 & 0 & 0 & 0 \\ 0 & 0 & 0 & J_a & 0 & 0 & 0 \\ 0 & 0 & 0 & 0 & J_r & 0 & 0 \\ 0 & 0 & 0 & 0 & 0 & J_b & 0 \\ 0 & 0 & 0 & 0 & 0 & 0 & J_q \end{bmatrix}, \quad \mathbf{B}_J = \begin{bmatrix} b_s & 0 & 0 & 0 & 0 & 0 & 0 \\ 0 & b_c & 0 & 0 & 0 & 0 & 0 \\ 0 & 0 & b_p & 0 & 0 & 0 & 0 \\ 0 & 0 & 0 & b_a & 0 & 0 & 0 \\ 0 & 0 & 0 & 0 & b_r & 0 & 0 \\ 0 & 0 & 0 & 0 & 0 & b_b & 0 \\ 0 & 0 & 0 & 0 & 0 & 0 & b_q \end{bmatrix}.$$

The stiffness and friction matrices $\mathbf{K}$ and $\mathbf{B}_K$ are:

$$\mathbf{K} = \begin{bmatrix} K_{sp} & 0 & 0 & 0 & 0 \\ 0 & K_{sa} & 0 & 0 & 0 \\ 0 & 0 & K_{pr} & 0 & 0 \\ 0 & 0 & 0 & K_{ab} & 0 \\ 0 & 0 & 0 & 0 & K_{bq} \end{bmatrix}, \quad \mathbf{B}_K = \begin{bmatrix} b_{sp} & 0 & 0 & 0 & 0 \\ 0 & b_{sa} & 0 & 0 & 0 \\ 0 & 0 & b_{pr} & 0 & 0 \\ 0 & 0 & 0 & b_{ab} & 0 \\ 0 & 0 & 0 & 0 & b_{bq} \end{bmatrix}.$$

As far as the considered two-stages planetary gear is concerned, the radius matrix $\mathbf{R}$ is defined in the following way:

$$\mathbf{R} = \begin{bmatrix} r_{s1} & -r_{cp} & r_p & 0 & 0 & 0 & 0 \\ r_{s2} & -r_{ca} & 0 & r_a & 0 & 0 & 0 \\ 0 & r_{cp} & r_p & 0 & -r_r & 0 & 0 \\ 0 & r_{ca} - r_{cb} & 0 & r_a & 0 & r_b & 0 \\ 0 & r_{cb} & 0 & 0 & 0 & r_b & -r_q \end{bmatrix}. \quad (10)$$

Radii r_i or r_{ij} present in matrix $\mathbf{R}$ are graphically defined in Fig. 10 and are constrained as follows:

$$\begin{aligned} r_{cp} &= r_p + r_{s1}, & r_{cb} &= 2r_a + r_b + r_{s2}, \\ r_{ca} &= r_a + r_{s2}, & r_q &= 2r_a + 2r_b + r_{s2}. \end{aligned}$$

The radii within matrix $\mathbf{R}$ defined in (10) have been computed by means of the rules defined in Sec. III-A. As an example, let us refer to element $r_{ab,c}$ which falls within the indirect contact case (see Fig. 5.b and 6.b). This represents a particular case, as the angular velocity $\vec{\omega}_c$ affects the force vector $\vec{F}_{ab}$ through two different intermediate gears, characterized by moments of inertia J_a and J_b. It follows that $r_{ab,c}$ is given by the linear combination of two radii:

- $\vec{\omega}_c$ affects $\vec{F}_{ab}$ through J_a, therefore it is $S_{F_{ab}} = 1$ and $S_{\omega_c} = 1$, meaning that $r'_{ab,c} = r_{ca}$;

- $\vec{\omega}_c$ affects $\vec{F}_{ab}$ through J_b, therefore it is $S_{F_{ab}} = -1$ and $S_{\omega_c} = 1$, meaning that $r''_{ab,c} = -r_{cb}$;

From which the overall radius $r_{ab,c}$ can be computed:

$$r_{ab,c} = r'_{ab,c} + r''_{ab,c} = r_{ca} - r_{cb}.$$

When $\mathbf{K} \to \infty$, see (2), the angular velocities satisfy relation $\mathbf{R}\,\boldsymbol{\omega} = \mathbf{0}$ and are constrained as follows:

$$\begin{cases} r_p\,\omega_p - r_{cp}\,\omega_c + r_{s1}\,\omega_s = 0 \\ r_a\,\omega_a - r_{ca}\,\omega_c + r_{s2}\,\omega_s = 0 \\ r_{cp}\,\omega_c + r_p\,\omega_p - r_r\,\omega_r = 0 \\ r_a\,\omega_a + r_b\,\omega_b + \omega_c(r_{ca} - r_{cb}) = 0 \\ r_b\,\omega_b + r_{cb}\,\omega_c - r_q\,\omega_q = 0 \end{cases} \tag{11}$$

In this case, by choosing $\mathbf{x}_1 = \begin{bmatrix} \omega_c & \omega_r \end{bmatrix}^{\mathrm{T}}$, from (11) one obtains the congruent state space transformation $\mathbf{x} = \mathbf{T}_1\mathbf{x}_1$ where $\mathbf{T}_1 = \begin{bmatrix} \mathbf{Q}_1 \\ \mathbf{0} \end{bmatrix} \mathbf{x}_1$ and matrix $\mathbf{Q}_1$ is defined as follows:

$$\mathbf{Q}_1 = \begin{bmatrix} 1 & 0 \\ \frac{r_{s1}}{2r_{cp}} & \frac{r_r}{2r_{cp}} \\ -\frac{r_{s1}}{2r_p} & \frac{r_r}{2r_p} \\ \frac{r_{ca}r_{s1} - 2r_{cp}r_{s2}}{2r_a r_{cp}} & \frac{r_{ca}r_r}{2r_a r_{cp}} \\ 0 & 1 \\ \frac{r_{cb}r_{s1} - 2r_{ca}r_{s1} + 2r_{cp}r_{s2}}{2r_b r_{cp}} & -\frac{2r_{ca}r_r - r_{cb}r_r}{2r_b r_{cp}} \\ \frac{r_{cb}r_{s1} - r_{ca}r_{s1} + r_{cp}r_{s2}}{r_{cp}r_q} & -\frac{r_{ca}r_r - r_{cb}r_r}{r_{cp}r_q} \end{bmatrix}$$

By using the congruent transformation $\mathbf{x} = \mathbf{T}_1\mathbf{x}_1$ to system (2), one obtains a reduced system having the same structure of the reduced model (7) obtained in the previous example. In this case, the analytical expressions of J_1, J_3 and J_2 in matrix $\mathbf{L}_1$, together with the analytical expressions of b_1, b_3 and b_2 in matrix $\mathbf{A}_1$, are not reported in this paper because they are too long. Even in this case, the force vector $\mathbf{F}$ can be recovered from the reduced POG model (7) by using (8).

A. Simulation results

The two-stages planetary gear has been simulated in Matlab/Simulink by using the following parameters:

```
r_r = 5.4*cm; r_s1 = 5.4*cm;% Ring and Sun_1 radii
r_s2 = 2.6*cm; r_p = 3.8*cm;% Sun_2 and Planetary radii
r_a  = 5.8*cm; r_b = 5*cm;  % Planet_a and Planet_b radii
r_cp= 9.2*cm; r_ca= 8.4*cm; % r_ca and r_cb radii
r_cb= 19.2*cm; r_q= 24.2*cm;% r_cb and r_q radii
J_c = 1.891*kg*meters^2;    % Carrier: inertia
J_p = 0.0038321*kg*meters^2;% Planetary_p: inertia
J_r = 0.0046882*kg*meters^2;% Ring: inertia
J_s = 0.0062509*kg*meters^2;% Sun: inertia
J_a = 0.020798*kg*meters^2; % Planetary_a: inertia
J_b = 0.011486*kg*meters^2; % Planetary_b: inertia
J_q = 2.5213*kg*meters^2;   % Ring_2: inertia
b_c = 0.64*Nm/rpm; b_p = b_c; b_r = b_c;
b_s = b_c; b_a = b_c; b_b = b_c; b_q = b_c;
K_sp = 1000*Newton/mm;      % Sun-Plan_p: stiffness
K_sa = K_sp; K_pr = K_sp; K_ab = K_sp; K_bq = K_sp;
b_sp = 8*Newton*s/cm;       % Sun-Plan_p: fric. coeff.
b_sa = b_sp; b_pr = b_sp; b_ab = b_sp; b_bq = b_sp;
Tau = [100 0 0 0 0 0 0]*Nm; % Input Torques
W_0 = [0 0 0 0 0 0 0]*rpm;  % Angular velocities: In. Co.
F_0 = [0 0 0 0 0]*Newton;   % Tangential forces: In. Co.
```

The angular velocities ω_i, for $i \in \{c, p, s, r, g, m\}$, are shown in Fig. 11; the tangential forces F_{ij}, for $ij \in \{ps, pr, sg, rm\}$, are shown in Fig. 12.

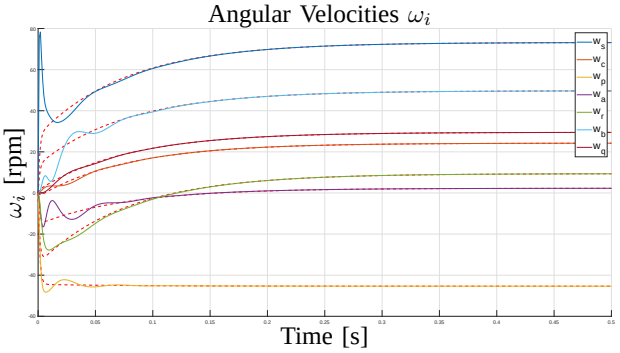

Fig. 11. Angular velocities ω_i, for $i \in \{s,\ c,\ p,\ a,\ r,\ b,\ q\}$.

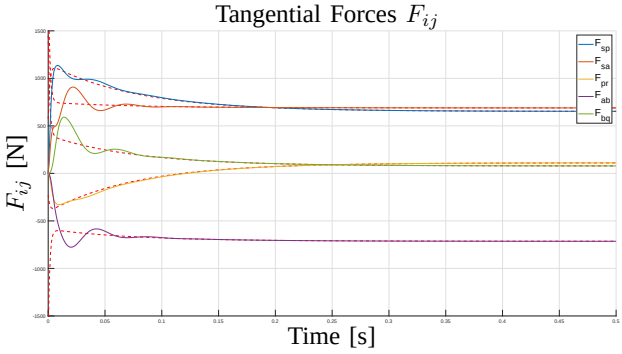

Fig. 12. Tangential forces F_{ij}, for $ij \in \{sp,\ sa,\ pr,\ ab,\ bq\}$.

V. Conclusions

In this paper, a new method for modeling planetary gear transmission systems has been presented. The method provides the user with both the full elastic model of the system and the reduced rigid one. The POG modeling technique allows the user to select the angular speeds to be kept as state variables in the reduced model. Moreover, the reduced model also provides the tangential elastic forces present between the gears. The presented modeling method has been tested on two different planetary gear systems, which have been modeled and simulated in Matlab/Simulink. The simulative results have been reported in this paper and show the effectiveness of the presented method.

References

[1] A. Mohsine, E. M. Boudi, A. E. Marjani, "Modeling and Structural Analysis of Planetary Gear of a Wind Turbine", International Renewable and Sustainable Energy Conference (IRSEC), Marrakech, Morocco, November 14-17, 2016.

[2] H. Jingnan, W. Shaohong, M. Chao, "Nonlinear dynamic analysis of 2K-H planetary gear transmission system", 13th IEEE International Conference on Electronic Measurement & Instruments (ICEMI), Yangzhou, China, October 20-22, 2017.

[3] Q. Tao, J. Zhou, W. Sun, J. Kang, "Study on the Inherent Characteristics of Planetary Gear Transmissions", 21st International Conference on Automation and Computing (ICAC), Glasgow, UK, Sept. 11-12, 2015.

[4] J. Liu, H. Peng, "Modeling and Control of a Power-Split Hybrid Vehicle", IEEE Trans. on Control Systems Technology, Nov. 2008.

[5] X. Zhang, H. Peng, J. Sun, S. Li, "Automated Modeling and Mode Screening for Exhaustive Search of Double-Planetary-Gear Power Split Hybrid Powertrains", ASME Dynamic Systems and Control Conference, San Antonio, Texas, Oct 22-24, 2014.

[6] R. Zanasi, "The Power-Oriented Graphs Technique: System modeling and basic properties", IEEE Vehicle Power and Propulsion Conference, Lille, France, Sept. 1-3, 2010.